Progress In Electromagnetics Research C, Vol. 133, 39–49, 2023

Study on Electromagnetic Exposure of High-Speed Railway Platform Staff Workers Induced by Contact Wires

Changqiong Yang* **and Mai Lu**

Abstract—The bodies of platform staff workers in high-speed railway stations absorb induction electric field when being exposed to the electric field environment of contact wires with 25 kV high-voltages. To analyze the safety of electromagnetic exposure of the station platform staff workers with different numbers of tracks, this paper establishes a model with 6 tracks, 2 platforms, and 4 staff workers on the platform simulating the actual situation. It then analyzes the distribution of induction electric field present in their human body tissues, which in the electric field environment is generated by the high voltages of the contact wires of 1 track, 3 tracks, 6 tracks, respectively. Calculation results show that the maximum induction electric field of staff worker on the platform with different track numbers appears at the scalp, and the electric field intensity levels in the skull and brain are relatively small. For example, on the two platforms with 6 tracks, the maximum induction electric field of the staff worker is found in the scalp, and the values are 58.86 times and 1688.52 times of those of the skull and brain, respectively. For the staff worker at the safety white line, the maximum induction electric field in a human central nervous system is 0.61 mV/m, which is far less than the basic limit of 100 mV/m occupational exposure in the International Commission on Non-Ionizing Radiation Protection (ICNIRP) guidelines. With the increase in the number of tracks, the maximum induction electric field of the staff also increases correspondingly at the same position. Research results can provide data reference for the formulation of electromagnetic protection and standards for high-speed railway platform staff workers.

1. INTRODUCTION

The high-speed train pantograph on the top of the carriage comes to touches with the contact wire in a traction power supply system to obtain power frequency and single-phase 25 kV high voltages, and the power energy drives the train forward. With the rapid development of high-speed railway, the contact wire of a traction power supply system is used increasingly, thereby increasingly causing wider distribution of the power frequency electromagnetic field caused by the contact wire. The existing research on low-frequency electromagnetic field has shown that extremely low frequency electromagnetic field can make premature infants gain weight [1], and low-frequency electromagnetic fields may increase the probability of children's suffering from leukemia [2], help tumor growth and development of [3], and affect the immune system [4, 5]. Exposure to specific low-frequency electromagnetic fields can inhibit the growth of cancer cells [6] and affect Primary Cultured Hippocampal Neurons [7]. The low-frequency pulsed electromagnetic field has been used to study the fracture mechanism and osteoporosis model of animals, and it has also been used to treat fracture, osteoporosis, and oral implant bone in clinical settings [8, 9]. Extremely low frequency electric and magnetic fields may be associated with Alzheimer's disease [10].

Received 25 March 2023, Accepted 12 May 2023, Scheduled 22 May 2023
* Corresponding author: Changqiong Yang (lily_yang05@163.com).
The authors are with the Key Laboratory of Opto-Electranic Technology and Intelligent Control, Ministry of Education, Lanzhou Jiaotong University, China.

People also increasingly pay more and more attention to the study of electric field distribution on railway platforms with people's attention to occupational or public health [11–13], such as the spatial distribution of electric field caused by catenary in electrified railway [14], the effects of wireless power transfer (WPT) systems on human health [15, 16], and the study of electromagnetic exposure result of transmission lines [17, 18].

Figure 1 shows the site of a high-speed railway platform.

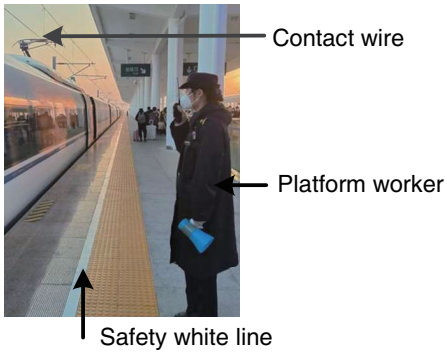

Figure 1. A high-speed railway platform.

In Fig. 1, a platform staff worker often stands within the safe white line when working. The distance from the edge of the platform to the center of the rail line is 1.75 m; the distance from the safe white line to the edge of the platform is 1 m; and the height of platform is 1.25 m.

The research on a platform power-frequency electric field environment is mainly based on the field measurement space. The study on the electromagnetic exposure of workers is mainly based on simulation calculation by establishing a two-dimensional human model. Paper [19] monitored and analyzed the distribution of power frequency electric field in a high-speed and a common speed electrified railway station. The results showed that the power frequency electric field intensity levels of high-speed and common speed platform are 0.176 kV/m–3.380 kV/m and 0.010 kV/m–1.779 kV/m, respectively, which is lower than the reference limit of 5 kV/m specified in the International Commission on Non-Ionizing Radiation Protection (ICNIRP) guidelines [20]. Song et al. [21] used a finite element analysis software to calculate the electric field and magnetic induction intensity by establishing the equivalent model, including the human body, catenary, train, and platform. The results showed that the electromagnetic field intensity is closely related to the horizontal distance from the monitoring point to the projection point of the contact line to the ground. At the white safety line, the maximum power frequency electric field shielding coefficients of the train to chest and head of the human body on the platform are 90.9% and 74.5%, respectively. In the space area of head, the maximum electric field intensity reaches 4.678 kV/m without a train. Jiang et al. [22] measured the electric field strength of the main platform in the CRH380B bullet train operation line of a Railway Administration. At the safety white line, the measurement results have shown that the maximum electric field intensities at the heights of 1.1–1.3 m and 1.5–1.7 m from the ground are 3.382 kV/m and 4.322 kV/m, respectively, without a train; the values are greater than the corresponding values when a train is parked. By using the electromagnetic simulation software, the finite element model of the catenary and standing and bending posture of the hydraulic worker was set up. On the power-frequency electromagnetic environment caused by the catenary in the high-speed railway station, Yuan et al. [23] analyzed the worker's occupational electromagnetic exposure level. The results showed that the intensity of the induction electric field and the density of the induction current in the tissues of the hydraulic worker's body with standing posture are greater than the corresponding values of the bending posture. The intensity of the induction electric field in the tissues of the hydraulic worker's body with standing posture is less than the basic limit of occupational electromagnetic exposure in the ICNIRP guidelines. Liu et al. [24] studied the distribution of electric field intensity caused by train and building by establishing a two-dimensional model including a high-speed railway platform, catenary, a train, and a building. The results showed that the shielding

effect of train was significantly greater than that of the building. At the white safety line, the shielding effects of the train and building were 86% and 6%, respectively, In the head space, the electric field intensity is close to 5 kV/m without a building and train.

At the high-speed railway station, a corresponding number of contact wires are distributed according to the number of tracks. Generally, the number of tracks in the high-speed railway station is more than that in the section (the section generally has up and down tracks). For example, the Lanzhou West Railway Station has total tracks of 28, while the Xi'an North Railway Station has 34. The more the number of tracks and contact wires is, the more complex the electromagnetic exposure is to the platform staff worker in the electric field environment caused by the high voltage of the contact wire. The electromagnetic exposure will cause a non-thermal effect on the human tissue self-regulation and self-recovery. It will cause permanent damage to the human tissue when the regulation and recovery function decrease and exceed the time of the self-recovery function of the human body. The health effect has aroused public concern caused by the complex electromagnetic environment in high-speed railway stations, but research scarcely exists on the electric field environment caused by multiple contact wires with different numbers of tracks and electromagnetic exposure of the platform worker. Therefore, studying the electromagnetic exposure of the platform worker at different scale stations with the electromagnetic environment caused by the contact wire with power frequency of 50 Hz and voltage of 25 kV has profound significance.

At present, most of the existing studies on the electromagnetic exposure dose analysis of human tissues under the transmission line [25] and contact wire [26] adopt the finite element method. Combining the research results of paper [21] and study [22], the electric field intensity on the platform tends to decrease when a train stopes there. Therefore, by using electromagnetic field theory and finite element simulation software, this paper calculates and analyzes the electric field distribution in the tissues of the platform worker's body in high-speed railway stations with different numbers of high voltage contact wires without a train. The research results have certain reference value for formulating the electromagnetic exposure standard of high-speed railway. It provides basis reference of electromagnetic protection for station operators. It will also help the public and professionals eliminate the risk of electromagnetic exposure and the health risks caused by contact wires with high voltage at the different scale stations.

2. MODEL PARAMETERS

Considering the requirements of simulation calculation for computer hardware, some simplified processing shall be carried out during the actual modeling. 1) The ground is a good conductor, and the platform, canopy, and rail are not considered in the model; 2) The catenary system only considers the contact wire; 3) The maximum number of tracks is 6. Fig. 2 shows the simulation model.

In Fig. 2, based on the actual size of a high-speed railway platform, tracks I and II are the main lines. The distance of corresponding contact wires is 7 m; the distance of contact wires corresponding to tracks I and 3 is 15.5 m; the distance of contact wires corresponding to tracks II and 4 is 15.5 m; the distance of contact wires corresponding to tracks 5 and 3 is 6 m; the distance of contact wires corresponding to tracks 4 and 6 is 6 m; the height of workers' feet on the platform from the ground is 1.25 m; the height of contact wire from the ground is 5.5 m; and the radius of contact wire is 6.6 mm [27]. The lower boundary of the air domain of the model coincides with the ground, and the potential is defined as 0 V. For the human body model, some scholars use the real digital human head model [28, 29], but its cost is too expensive. In this paper, the height of the platform worker model is 1.75 m [30] according to the international adult body proportion. The tissues of human body primarily make up the brain, skull, scalp, and torso. Fig. 3 shows the human body model.

The relative permittivity and conductivity of brain consist of the average values of brain white matter, brain gray matter, and cerebrospinal fluid. The average values of muscle, cortical bone, and fat are used as the trunk dielectric parameters. At frequency of 50 Hz, Table 1 shows the dielectric constants of human tissues.

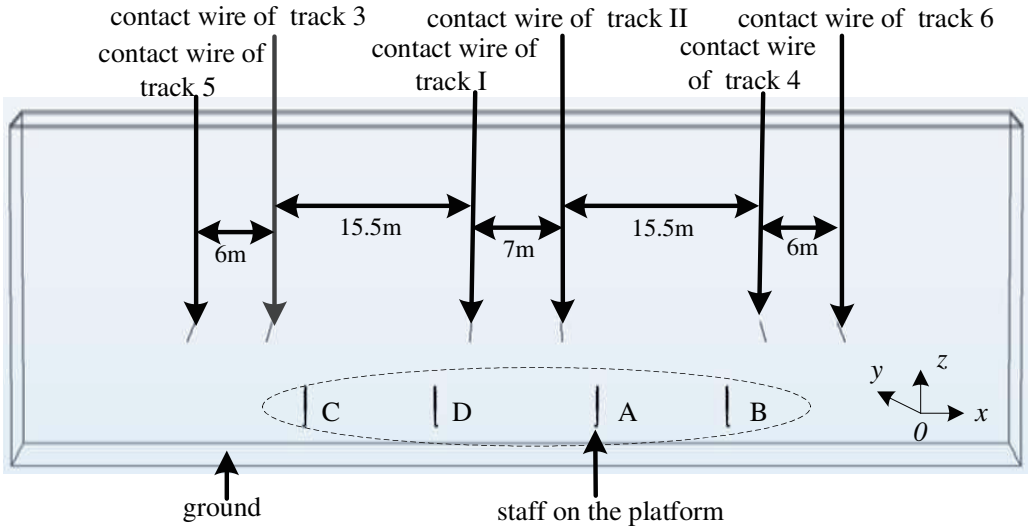

Figure 2. High-speed railway platform.

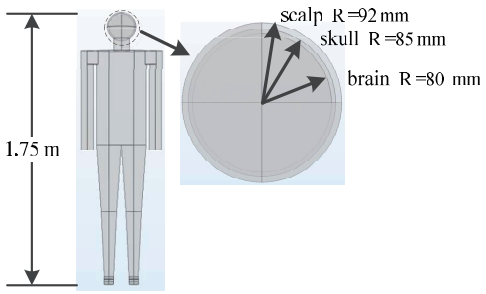

Figure 3. Human model.

Table 1. Dielectric parameters of human tissues at frequency of 50 Hz [31].

Tissues	**Relative permittivity ε_r**	**Electric Conductivity σ (S/m)**
Scalp (Skin wet)	5.13×10^4	4.27×10^{-4}
Skull (Bone cortical)	8.87×10^3	2.01×10^{-2}
Brain	5.80×10^6	7.09×10^{-1}
Trunk	6.40×10^6	1.51×10^{-1}
Cerebro spinal fluid	1.09×10^2	2.00×10^0
Brain grey matter	1.21×10^7	7.50×10^{-2}
Brain white matter	5.29×10^6	5.33×10^{-2}
Muscle	1.77×10^7	2.33×10^{-1}
Bone cortical	8.87×10^3	2.01×10^{-1}
Fat	1.47×10^6	1.96×10^{-2}

3. VALIDATION OF THE MODEL

To test the accuracy of the model, the equivalent charge method is used to calculate the spatial electric field intensity at different heights between the contact wire and the ground [32], and the theoretical calculated results are compared with the electric field intensity calculated by the simulated version in COMSOL Multiphysics to verify the accuracy of the model. Fig. 4 shows the calculation geometry.

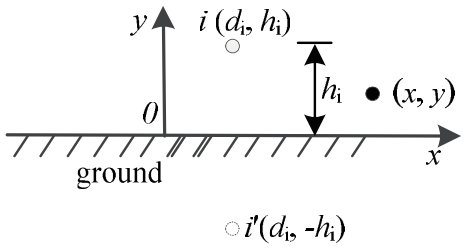

Figure 4. Geometry used for calculation of the electric field.

In Fig. 4, i represents the contact wire i with coordinates (d_i, h_i), and i' represents the mirror image corresponding to contact wire i with coordinates (d_i, $-h_i$). The potential coefficient P_{ii} can be written as the following Equation (1):

$$P_{ii} = \frac{1}{2\pi\varepsilon_0} \ln \frac{2h_i}{R_i}, \tag{1}$$

where $\varepsilon_0 = 1/(36\pi) \times 10^{-9}$ F/m; h_i is the height between the contact wire and the ground, m, and R_i is the radius of contact wire, m.

After the potential shift coefficient matrix $\mathbf{P}$ is obtained, the equivalent analog charge quantity $\mathbf{Q}$ is calculated by Equation (2) [33, 34] as follows.

$$Q = P_{ii}^{-1} \times V, \tag{2}$$

where Q is charge, C/m; V is potential, V.

According to Equations (1) and (2), after calculating the equivalent charge per unit length of the contact wire, the electric field intensity E at any point (x, y) in the space around the contact wire can be expressed as Equation (3).

$$\begin{cases} E_x = \dfrac{1}{2\pi\varepsilon_0} Q \left[\dfrac{x-d_i}{(x-d_i)^2+(y-h_i)^2} - \dfrac{x-d_i}{(x-d_i)^2+(y+h_i)^2} \right] \\ E_y = \dfrac{1}{2\pi\varepsilon_0} Q \left[\dfrac{y-h_i}{(x-d_i)^2+(y-h_i)^2} - \dfrac{y+h_i}{(x-d_i)^2+(y+h_i)^2} \right] \\ E = \sqrt{E_x^2+E_y^2} \end{cases}, \tag{3}$$

The radius of the contact wire is 6.6 mm; the height between contact wire and the rail surface is 5.5 m; and its effective value of voltage is 25 kV. Based on Equations (1) to (3), the electric field intensity at 4.5 m above the ground directly below the contact wire is calculated, and the value is 3.707 kV/m. In Fig. 2, only the contact wire of station track II is reserved, and the current interface in COMSOL Multiphysics is used for simulation calculation according to Equations (4) to (6).

$$\nabla \times \mathbf{J} = \mathbf{Q}_{j,v}, \tag{4}$$

$$\mathbf{J} = \sigma\mathbf{E} + \mathbf{j}\omega\mathbf{D} + \mathbf{J}_e, \tag{5}$$

$$\mathbf{E} = -\nabla\varphi, \tag{6}$$

where $\mathbf{J}$ is the current density, A/m^2; $\mathbf{Q}_{j,v}$ is the current source, A/m^3; σ is the conductivity, S/m; $\mathbf{E}$ is the electric field intensity, V/m; $\mathbf{J}_e$ is the external current density, A/m^2; and φ is the potential, V.

The simulation value of electric field intensity at 4.5 m above the ground directly and below the contact wire is 3.709 kV/m. The error between simulation calculation and theoretical calculation is 0.05%, which proves that the model can meet the required engineering calculation accuracy.

4. ELECTRIC FIELD INTENSITY OF HUMAN TISSUE ON SINGLE TRACK PLATFORM

To calculate the distribution of the space electric field, only the contact wire of track II is reserved in Fig. 2. The height measurements of the human head and chest are 1.5 m–1.7 m and 1.1 m–1.3 m, respectively. Thus, we cut off 6 lines, where the horizontal direction of −5 m to 5 m in the $x0z$ plane of $y = 0$, and the vertical height measurements are 2.35 m, 2.45 m, 2.55 m, 2.75 m, 2.85 m, and 2.95 m, respectively. Fig. 5(a) shows the cut-off lines, and Fig. 5(b) shows the corresponding electric field strength values of each line.

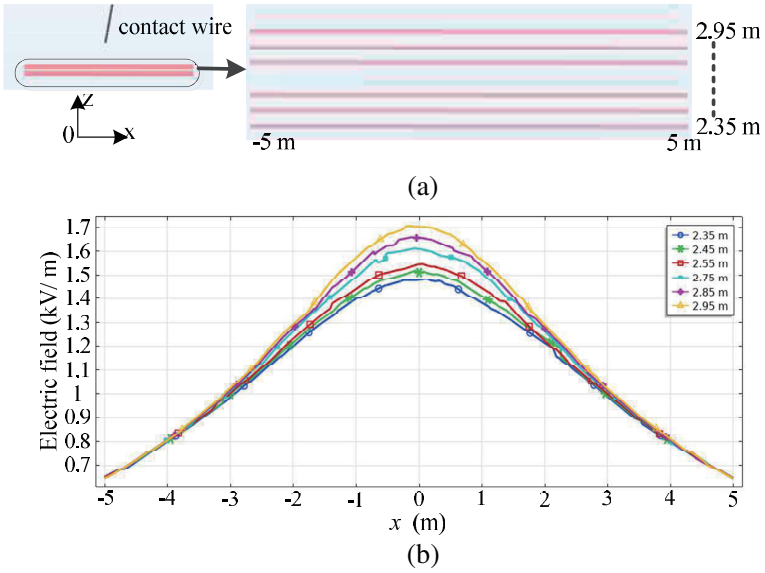

Figure 5. Electric field intensity at different heights: (a) Diagram of cut-off lines; (b) values of each line.

As shown in Fig. 5(b), the maximum electric field intensity appears directly below the contact wire. In the vertical direction, the closer the location is to the contact wire, the greater the electric field intensity is. The distribution trend of electric field intensity in the horizontal direction is the same at different heights. In the horizontal direction, with the location farther away from the contact wire, the electric field strength gradually weakens, and the attenuation speed also weakens. At distances of 3 m to 5 m in the horizontal position and 2.35–2.95 m from the ground, the electric field intensities are close to each other and have little change.

To analyze the electric field intensity distribution of the human tissue of the platform worker, only the contact wire of track II and the worker on the platform are reserved in Fig. 2. Through simulation calculation, Fig. 6(a) shows the distribution of electric field vector in human tissue, and Fig. 6(b) shows the distribution of the electric field intensity in the tissues.

Figure 6(a) shows that the vector of electric field in the human body flows from the top of head to foot. In Fig. 6(b), the maximum value of the electric field intensity of human internal tissues is 714 mV/m; the electric field is distributed in the head and rapidly decays from head to foot. Combination of Figs. 5(b) and 6(b) shows that the electric field intensity decays rapidly inside the worker's tissue mainly because the worker's bodily tissues and air are two different dielectric materials. In the normal direction, the electric field distribution is discontinuous on the whole materials boundary. The electrostatic induction charge is mainly distributed on the outermost surface of the worker's skin. To further observe the distribution of electric field intensity in the human head, the mid-cross sections of the high-signal operator's head are as follows: the coronal plane ($x = 2.75$ m, $y0z$ plane), the sagittal plane ($y = 0$ m, $x0z$ plane), and the axial plane ($z = 2.908$ m, $x0y$ plane). Fig. 9 shows the distribution of electric field inside the head.

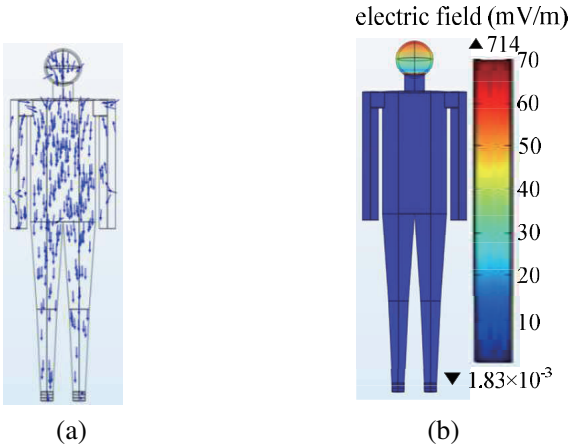

Figure 6. Distribution in human tissues: (a) electric field vector; (b) electric field intensity.

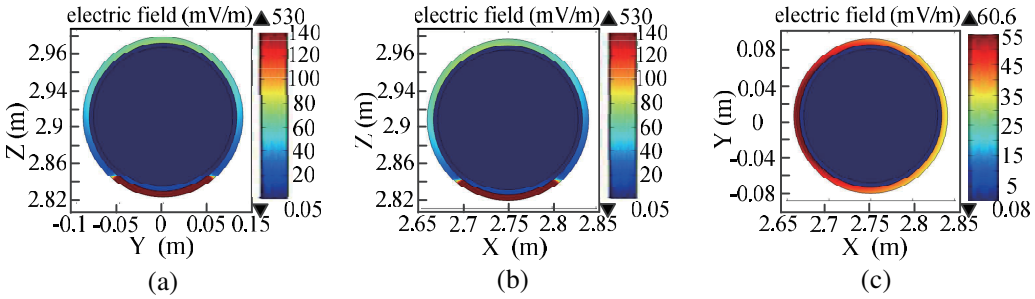

Figure 7. Electric field intensity distribution in different plane of the human head: (a) coronal plane; (b) sagittal plane; (c) axial plane.

As shown in Fig. 7, the distributions of electric field intensity in the sagittal plane and coronal plane of the head are similar, and the maximum value is 530 mV/m. The electric field is mainly distributed in the scalp near the neck because the scalp tissue near the neck collects induced charges in this strong electric field. The electric field intensity of the head axial plane is symmetrically and uniformly distributed along the Y axis, and the maximum value is 60.6 mV/m. Additionally, it is distributed at the scalp because the induction electrostatic charge is mainly distributed on the outermost surface of the human body. Fig. 7 shows that the scalp has strong electric field intensity at different planes of the head, whereas the electric field intensity levels in the skull and brain are relatively small, indicating that the scalp effectively protects the skull and brain.

5. EVALUATION OF HUMAN ELECTROMAGNETIC EXPOSURE AT MULTI-TRACK PLATFORM

Generally, high-speed railway stations have multiple tracks. Considering that the distance between tracks with platforms is much wider than that between tracks without platforms, the influence of the induction electric field in the platform worker varies. Therefore, we analyze the induction electric field of the workers' bodies standing on both sides of the platform with three tracks and two platforms with six tracks, respectively.

5.1. Analysis of Electromagnetic Exposure of Two Workers on a Platform

In Fig. 2, three contact wires of track II, track 4, and track 6 are loaded at 50 Hz and 27.5 kV, and the electromagnetic exposure of staff workers A and B are considered. After analysis and calculation,

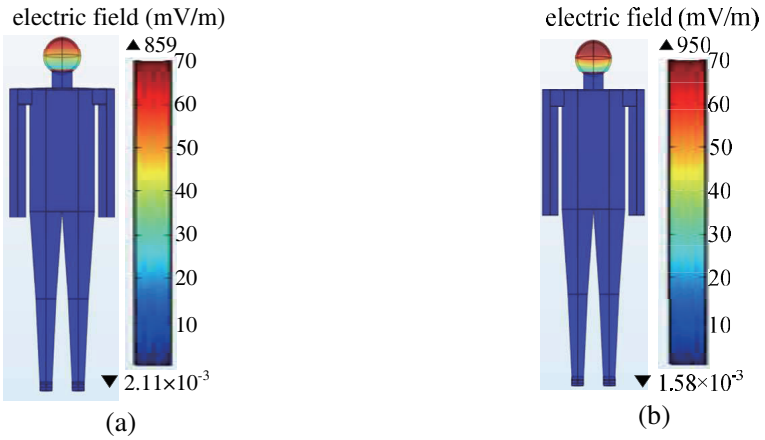

Figure 8. Distribution of electric field intensity in the human body (One platform): (a) worker A; (b) worker B.

Fig. 8 shows the distribution of electric field intensity in the internal tissues of staff A and B.

As shown in Fig. 8, the distribution values of electric field intensity in the human body of staff workers A and B at the same platform are similar, with values mainly distributed in the head and relatively small distribution in the trunk. The maximum electric field intensity levels inside the human body of staff workers A and B are 859 mV/m and 950 mV/m, respectively. The maximum value of the induction electric field of the staff A on the platform with 3 tracks is 145 mV/m higher than that on the platform with one track, but the distribution values of the induction electric field in the human tissue are similar.

5.2. Analysis of Electromagnetic Exposure of Four Workers on Two Platforms

In Fig. 2, six contact wires of track II, track 4, track 6, track I, track 3 and track 5 are simultaneously loaded at 50 Hz and 27.5 kV and four workers (A, B, C, and D) on two platforms. Fig. 9 shows the distribution of electric field internal human tissues.

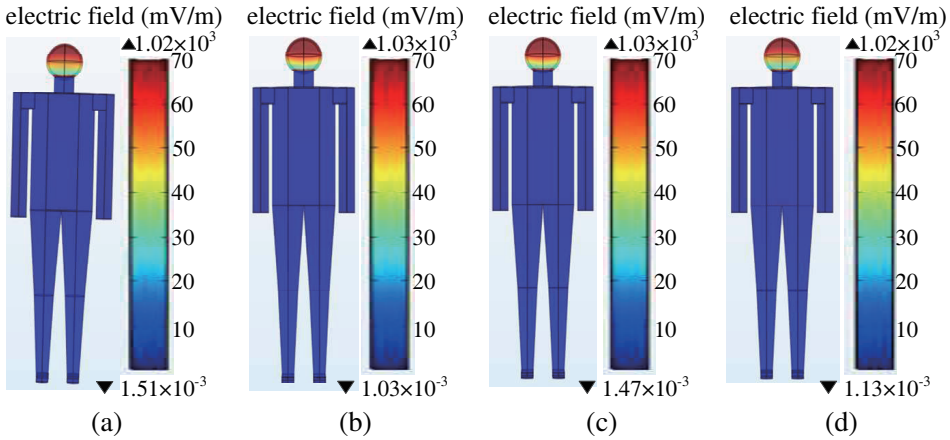

Figure 9. Distribution of electric field intensity in the human body (two platforms): (a) worker A; (b) worker B; (c) worker C; (d) worker D.

As shown in Fig. 9, the maximum electric field intensity levels of human tissues of two workers A and D are equal, and the value is 1.02 V/m. Those of workers B and C are equal, with a value of 1.03 V/m. The maximum electric field intensity of the four workers appeared in the head, because the human head tissues of the workers are closest to the contact wires, and the maximum electric field

intensity of the four staff members only differs by 0.01 V/m. Compared with Fig. 8, the distribution values of electric field intensity in human tissues of workers are similar, and the electric field intensity attenuates rapidly in the trunk. At the same location, the maximum values of human tissues of workers A and B increased by 161 mV/m and 80 mV/m, respectively. This finding indicates that the more the tracks (contact wires) are, the stronger the induction electric field is inside the worker's body.

To assess the health risk of electromagnetic exposure of workers under the most adverse conditions, the maximum electric field intensity values of each tissue of worker B in Figs. 8 and 9 are selected for analysis. Table 2 shows the values of the induction electric field at different parts of the body.

Table 2. Maximum electric field intensity values in the human tissues of worker B.

number of platforms	**electric field intensity (mV/m)**					
	in human tissues				**ICNIRP's basic limits**	
	scalp	**skull**	**brain**	**trunk**		
one platform	950	16.2	0.57	7.91	**CNS**	**AHB**
two platforms	1030	17.5	0.61	8.48	100	800

Notes: central nerve stimulation (CNS); All tissues of head and body (AHB)

At a frequency of 50 Hz, in the guidelines formulated by ICNIRP, the basic limits of occupational electromagnetic exposure of the central nervous system of the human body's internal tissues and the electric field intensity of the whole human body are 100 mV/m and 800 mV/m, respectively. From Table 2, the maximum value of electric field intensity can be concluded to distribute on the scalp, and the values exceed the basic occupational limit of 18.75% and 28.75%, respectively. Whether these values have an impact on human tissue health or not needs research through epidemiological investigation. Using the brain replacement of the central nervous system, the induction electric field of the worker's central nervous system is less than the basic limit of occupational exposure in the ICNIRP guidelines. In actual work, workers are often within the safe white line. When worker B is standing within 2 m of the safety white line in the station with 6 tracks, the maximum electric field intensity at the scalp is 793 mV/m, which is lower than the basic occupational exposure limit in ICNIRP guidelines.

6. CONCLUSIONS

This paper simulates and calculates the distribution of induction electric field inside the worker on the platform, which is the station with 3 tracks and 6 tracks, and the contact wires are loaded at 50 Hz and 27.5 kV. The following conclusions are obtained through performed numerical analysis:

1) The distribution of spatial electric field shows that the maximum value is directly below the contact wire, and its values gradually decrease as the vertical or horizontal distance increases from the contact wire.
2) At the safety white line, the maximum value of the induction electric field inside the worker's body appears on the scalp, and the maximum value exceeds 28.75% of the basic occupational limit in the ICNIRP guidelines. Whether this value has an impact on the health of human tissues still needs research through epidemiological investigation.
3) The maximum induction electric field by the human central nervous system at the safety white line is 0.61% of the basic limit of occupational exposure in the ICNIRP guidelines.
4) The research results can provide data reference for electromagnetic protection and standard formulation of high-speed railway for platform workers.

ACKNOWLEDGMENT

The authors would like to acknowledge the financial support by the National Natural Science Foundation of China (Grant No. 51867014) and by the Department of Education of Gansu Province under Grant 2022A-046. We are grateful for the peer reviewers who gave valuable comments during reviewing the manuscript.

REFERENCES

1. Lee, C. Y., J. Y. Tang, P. J. Chen, L. S. Jang, and Chuang H. L., "The effect of extremely low frequency electromagnetic field on weight gain of preterm babies," *2020 IEEE International Conference on Consumer Electronics-Taiwan (ICCE-Taiwan*), 1–2, Taoyuan, China, 2020.
2. Wertheimer, N. and E. Leeper, "Electrical wiring configurations and childhood cancer," *American Journal of Epidemiology*, Vol. 109, No. 3, 273–284, 1979.
3. Qi, G. G., X. X. Zuo, L. H. Zhou, E. Aoki, A. Okamula, M. Watanebe, H. P. Wang, Q. H. Wu, H. L. Lu, H. Tuncel, H. Watanabe, S. Zeng, and F. Shimamoto, "Effects of extremely low-frequency electromagnetic fields (ELF-EMF) exposure on B6C3F1 mice," *Environment Health Preventive Medicine*, Vol. 20, No. 4, 287–293, 2015.
4. Bao, J., "Health effects of extremely low frequency electromagnetic fields," *High Voltage Engineering*, Vol. 41, No. 8, 2550–2561, 2015.
5. Mahaki, H., H. Tanzadehpanah, N. Jabarivasal, K. Sardanian, and A. Zamani, "A review on the effects of extremely low frequency electromagnetic field (ELF-EMF) on cytokines of innate and adaptive immunity," *Electromagnetic Biology and Medicine*, Vol. 38, No. 1, 84–95,2019.
6. Wang, M. H., K. W. Chen, D. X. Ni, H. Fang, L. S. Jang, and C. H. Chen, "Effect of extremely low frequency electromagnetic field parameters on the proliferation of human breast cancer," *Electromagnetic Biology and Medicine*, Vol. 40, No. 3, 384–392, 2021.
7. Zeng, Y., Y. Y. Shen, L. Hong, Y. F. Chen, X. F. Shi, Q. L. Zeng, and P. L. Yu, "Effects of single and repeated exposure to a 50-Hz 2-mT electromagnetic field on primary cultured hippocampal neurons," *Neuroscience Bulletin*, Vol. 33, No. 3, 299–306, 2017.
8. Sharrard, W., "A double blind trial of pulsed electromagnetic fields for delayed union of tibial fractures," *Journal of Bone and Joint Surgery*, Vol. 72, No. 3, 347–355, 1990.
9. Giordano, N., E. Battisti, S. Geraci, M. Fortunato, C. Santacroce, M. Rigato, L. Gennari, and C. Gennari, "Effect of electromagnetic fields on bone mineral density and biochemical marker soft bone turnover in osteoporosis: a single-blind, randomized pilot study," *Current Therapeutic Research*, Vol. 62, No. 3, 187–193, 2001.
10. Mara, H., G. Priyanka, K. Daniel, and H. Riadh, "Scoping review of the potential health effects of exposure to extremely low-frequency electric and magnetic fields," *Critical Reviews in Biomedical Engineering*, Vol. 47, No. 4, 323–347, 2019.
11. Li, J. and M. Lu, "Safety assessment of electromagnetic exposure for adult and child passengers standing on the subway platform," *Archives of Electrical Engineering*, Vol. 71, No. 3, 755–773, 2022.
12. Travassos, X. L., S. L. Avila, S. Grubisic, A. Linhares, and N. Ida, "Electromagnetic field exposure assessment in a multi source telecommunication environment: Application to nonoccupational exposure in public spaces," *Wireless Personal Communications*, Vol. 110, No. 4, 2213–2225, 2020.
13. Ghnimi, S. and A. Gharsallah, "The potential effect of low-frequency EM fields on the human body," *Journal of Electrical Systems*, Vol. 16, No. 1, 119–130, 2020.
14. Zhou, H. W., Q. Yue, Z. Qiu, and L. P. Sun, "Calculation of electric field distribution caused by electrified railway catenary," *Electric Machines and Control*, Vol. 18, No. 8, 81–86, 2014.
15. Agcal, A., T. H. Dogan, and G. Dogan, "The effects of operating frequency on wireless power transfer system design and human health in electric vehicles," *Electrical*, Vol. 22, No. 2, 188–197, 2022.
16. Mou, W. T. and M. Lu, "Research on shielding and electromagnetic exposure safety of an electric vehicle wireless charging coil," *Progress In Electromagnetics Research C*, Vol. 117, 55–72, 2021.
17. Korobsova, V., Y. Morozov, and M. Stolorov, "Influence of the electric field in 500 and 750 kV switchyards on maintenance staff and means for its protection," *International Conference on High-tension Electric Systems*, 23–26, CIGRE, Paris, France, 1972.
18. Yamina, B. and Y. Nabil, "Assessment of magnetic field induced by overhead power transmission lines in Algerian National Grid," *Electrical Engineering*, Vol. 104, No. 2, 969–978, 2022.

19. Huang, Z. H., "Investigation and analysis of power frequency electric field of a high-speed railway and ordinary speed railway," *Railway Energy Saving & Environmental Protection & Occupational Safety and Health*, Vol. 5, No. 2, 75–76, 2015.
20. ICNIRP, "Guidelines for limiting exposure to time-varying electric and magnetic fields (1 Hz to 100 kHz)," *Health Physics*, Vol. 99, No. 6, 818–836, 2010.
21. Song, C. W., M. G. Liu, X. Wang, H. Tian, and W. Li, "Analysis of electromagnetic environment around high-speed railway platform," *Electric Drive for Locomotives*, No. 6, 50–54, 66, 2018.
22. Jiang, H. Z., Y. X. Qiu, Q. Wang, X. H. Chen, and X. Y. Zhang, "Research on power frequency electric field of high-speed railway station and train carriages," *Railway Energy Saving & Environmental Protection & Occupational Safety and Health*, Vol. 4, No. 5, 236–239, 2014.
23. Yuan, X., R. Tian, and M. Lu, "Research on radiation of power frequency electric field in high-speed railway station catenary to workers," *Advanced Technology of Electrical Engineering and Energy*, Vol. 41, No. 5, 80–88, 2022.
24. Liu, S. B., W. Liu, L. C. Song, and W. J. Guo, "Research on spatial electric field distribution of high-speed railway station under AT power supply model," *Computer Simulation*, Vol. 39, No. 1, 111–115, 2022.
25. Shiina, T., T. Kudo, D. Herai, Y. Kuranari, Y. Sekiba, and K. Yamazaki, "Calculation of internal electric fields induced by power frequency magnetic fields during live-line working using human models with realistic postures," *IEEE Transactions on Electromagnetic Compatibility*, Vol. 63, No. 6, 1812–1819, 2021.
26. Tian, R. and M. Lu, "Safety assessment of electromagnetic exposure in high-speed train carriage with full passengers," *Annals of Work Exposures and Health*, Vol. 64, No. 8, 838–851, 2020.
27. Zhang, J. Q. and M. L. Wu, "Calculation method of OCS ampacity for electric railway" *Journal of the China Railway Society*, Vol. 37, No. 12, 40–45, 2015.
28. Lu, M. and S. Ueno, "Comparison of the induced fields using different coil configurations during deep transcranial magnetic stimulation," *Plos One*, Vol. 12, No. 6, e0178422, 2017.
29. Lu, M. and S. Ueno, "Safety assessment of H-coil for nursing staff in deep transcranial magnetic stimulation," *IEEE Magnetics Letters*, Vol. 13, 1–5, 2022.
30. Alvin, R. T., *Ergonomics Diagram-Human Factors in Design*, translated by Zhu T., China Architecture & Building Press, 1998.
31. Andreuccetti, D., R. Fossi, and C. I. Physics, "An internet resource for the calculation of the dielectric properties of the body tissues in the frequency range 10 Hz–100 GHz," *IFAC-CNR, Florence (Italy)*, 1997, based on data published by C. Gabriel et al. 1996, [Online]. Available:http://niremf. ifac. cnr.it/tissprop/.
32. Zhang, Y. Y., A. H. Wang, W. W. Yang, N. N. Gao, L. Niu, P. Li, and J. X. Huang, "Calculation of power frequency electric field around ultra-high voltage AC transmission lines," *IOP Conference Series: Materials Science and Engineering*, Vol. 486, No. 1, 2019.
33. Keikko, T., J. Isokorpi, and L. Korpinen, "Practical problems in calculating electric fields of transmission lines," *Eleventh International Symposium on High Voltage Engineering*, 103–106, London, UK, 1999.
34. Bidi, M., "Biological risk assessment of high-voltage transmission lines on worker's health of electric society," *Archives of Electrical Engineering*, Vol. 69, No. 1, 57–68, 2020.